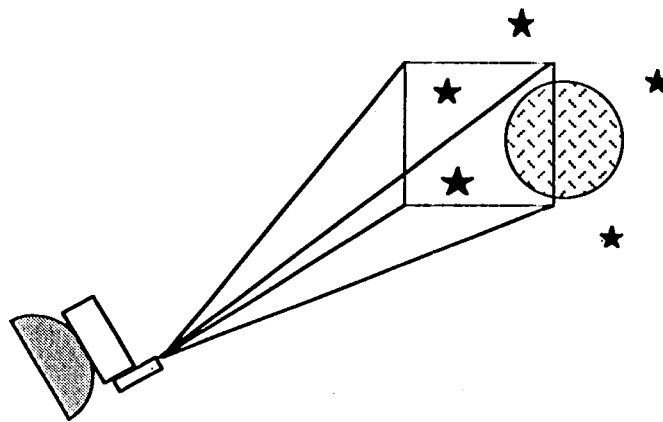




AUTONOMOUS OPTICAL NAVIGATION FOR THE PLUTO FAST FLYBY MISSION

Robin M. Vaughan and Stephen P. Synnott

Jet Propulsion Laboratory
California Institute of Technology
Pasadena, California, USA



AAS/AIAA Astrodynamics Specialist Conference

HALIFAX, NOVA SCOTIA, CANADA

14-17 AUGUST 1995

AAS Publications Office, P.O. Box 28130, San Diego, CA 92198

AUTONOMOUS OPTICAL NAVIGATION FOR THE PLUTO FAST FLYBY MISSION

Robin M. Vaughan* and **Stephen P. Synnott†**

This paper discusses an autonomous optical navigation capability to be added to the spacecraft flight system for a Pluto flyby mission. This system uses the spacecraft camera and new flight software to improve knowledge of the spacecraft's Pluto-relative trajectory in the last few days before encounter. A series of pictures containing images of Pluto against the star background are shuttered and processed to obtain increasingly accurate estimates of the actual time of closest approach. Start times for designated blocks of science observations around closest approach are shifted based on these estimates so that they begin at the desired time relative to the true closest approach. This simple time shift restores the geometry assumed in the original observation designs, providing higher confidence that the desired data will be captured. The paper presents a prototype design for the new flight software that extracts the navigation information from the optical navigation pictures. Implementations of image processing and orbit determination functions are described in detail. Overall system performance is illustrated by processing a series of pictures simulated along a typical Pluto flyby trajectory.

INTRODUCTION

Pluto and its moon Charon are the only major planetary system as yet unexplored by robotic spacecraft. Numerous proposals for missions to Pluto have been considered in recent years. JPL is currently studying a mission called Pluto Express. Its predecessor, the Pluto Fast Flyby mission, was under development until the fall of 1994. These missions have many common features. Most importantly for this paper, they have similar encounter geometries. Both are flyby missions with essentially linear trajectories relative to Pluto and large approach velocities in the range of 15-20 km/sec. It is this flyby geometry that ultimately dictates the addition of autonomous optical navigation capability to the spacecraft flight system.

The importance of optical navigation (OPNAV) for a Pluto mission was discussed in (Ref. 1). A combination of traditional, ground-based techniques and a new autonomous system is necessary to meet the navigation requirements. Standard techniques are applied in a "far encounter" phase covering the period from 6 months to a few days before closest approach to Pluto. The pictures taken in this phase are returned to earth for processing and incorporated in orbit determination solutions along with radiometric data. Due to errors in the Pluto ephemeris, however, there is still a large uncertainty in the time-of-flight, or downtrack, direction at the end of this phase. This uncertainty must be reduced in order to obtain the desired science observations around closest approach. Optical navigation pictures taken closer to encounter can provide this reduction. Constraints imposed by the flyby geometry and the spacecraft flight system, along with the long one-way light time at Pluto, preclude the return of these later pictures for ground processing. An on-board optical navigation

* Member of the Technical Staff, Jet Propulsion Laboratory, California Institute of Technology, Pasadena, CA.

† Technical Group Supervisor, Jet Propulsion Laboratory, California Institute of Technology, Pasadena, CA

system is therefore activated to obtain and process pictures in a "near encounter" phase starting a few days and ending just a few hours before closest approach.

This paper describes the prototype Autonomous Optical Navigation System (AONS) originally developed for the Pluto Fast Flyby mission. First, an overview of the operation of AONS during the Pluto encounter is given. The integration of the system within the overall mission scenario is discussed and the necessary functionality is identified. The resulting prototype design is then presented. The high-level system architecture is described, including a summary of information flow between the major blocks of the system. Next, the functions of each major block are described in detail, including derivation of key equations. The performance of the prototype AONS is then demonstrated by application to a sample Pluto mission trajectory.

OPERATIONAL SCENARIO

The optical data measure the spacecraft's Pluto-relative position in a plane perpendicular to the line-of-sight from the spacecraft to Pluto, called the image plane. For the linear Pluto trajectories of PFF and Pluto Express, the line-of-sight is essentially parallel to the approach velocity vector until a few days before closest approach and the image plane nearly coincides with the B-plane used for navigation targeting.[†] Pictures taken in the far encounter period therefore provide an excellent measurement of the spacecraft's B-plane aimpoint, but are relatively insensitive to errors in the downtrack direction. This leads to a long, narrow navigation error ellipsoid for the last ground-based orbit determination solution as shown in Figure 1 (a). The dominant error, corresponding to the largest axis of the ellipsoid, is in the radial or downtrack direction. As the spacecraft moves closer to Pluto, the line-of-sight direction rotates away from the approach velocity vector, allowing the optical data to measure the downtrack position, as shown in Figure 1(h). The sensitivity to downtrack error becomes significant within 2-3 days of closest approach, with the most dramatic increase coming within the last 24 hours.

The schedule for acquiring optical navigation pictures with the autonomous system is driven by the rate of improvement in the optical data's ability to measure downtrack position in the near encounter period. Pictures are sparsely distributed early in the period, where the viewing geometry changes more slowly. A typical schedule calls for one OPNAV picture to be taken and processed approximately every 8 hours between 3 days and 40 hours before closest approach. The frequency of OPNAV pictures increases starting at about 40 hours before closest approach. These later observations are typically separated by only 1-2 hours to track the more rapid increase in sensitivity of the optical measurements. The pictures taken in the last day are the most critical to successful performance of AONS. The accuracy of the downtrack position estimate depends directly on how near to closest approach the last OPNAV picture can be shuttered and successfully processed. Initial studies have assumed the last picture is taken at about 4 hours before closest approach. Overall, a total of 10-20 pictures will be taken and processed by AONS.

Shuttering of the near encounter OPNAV pictures and subsequent processing by AONS will be triggered by pre-loaded time-tagged commands included in the spacecraft's sequence load(s). These observations must be integrated into the overall schedule of spacecraft science and engineering activities. The early, sparsely distributed pictures can easily be accommodated since science activity is also fairly low at this time. The later, more frequent pictures must be selected from specific opportunities when Pluto can be viewed against different groups of known background stars. These opportunities will occur at irregular intervals due to the rapidly changing viewing geometry. Integration of these observations into the overall schedule will be more challenging since science observations and their supporting engineering activities will be more frequent closer to encounter. A data cutoff at 4 hours before closest approach represents one possible compromise between the desired accuracy of the downtrack position estimate and the number of science observations that can be scheduled in the last few hours before closest approach.

[†] See the appendix of (Ref. 6) for a definition of the B-plane.

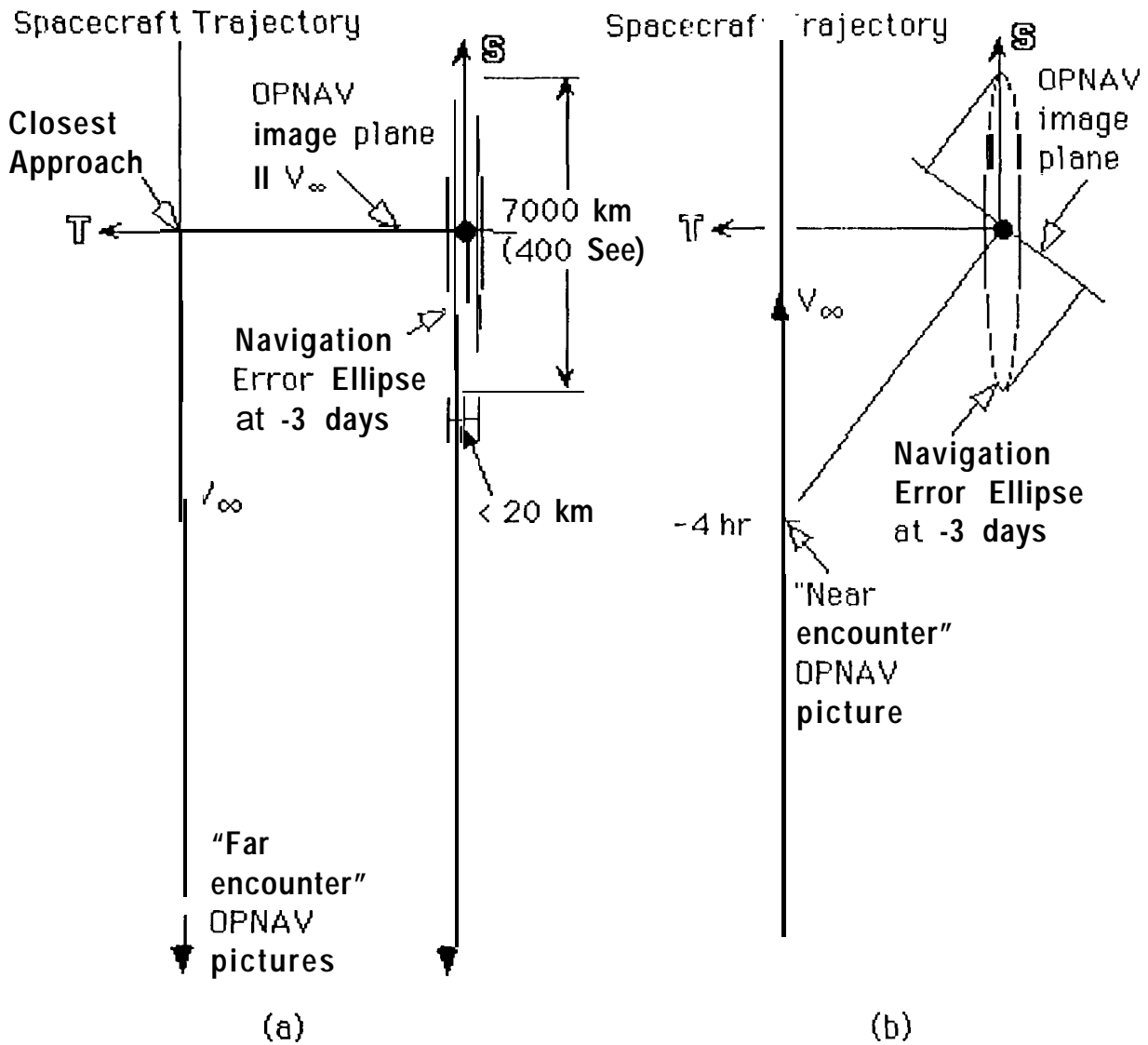


Figure 1: Increasing sensitivity of optical navigation data to downtrack position changes. Changes in downtrack position have larger projections onto the OPNAV image plane as the spacecraft moves nearer to Pluto.

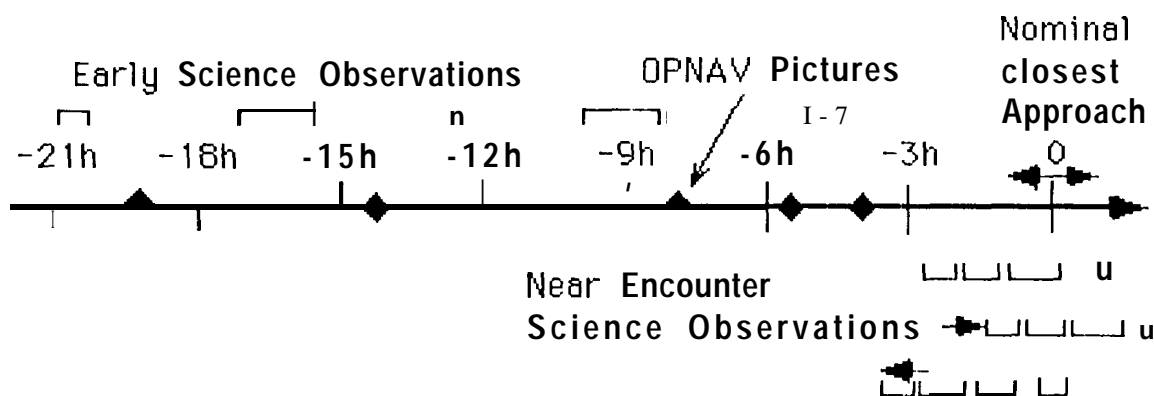


Figure 2: Operation of AONS. Science observation start times are shifted using estimate of closest approach time from OPNAV pictures.

AONS' primary responsibility is to improve knowledge of the spacecraft's Pluto-relative trajectory. It begins operation with the knowledge captured in the last ground-based orbit determination solution. The dominant error in this solution is in the clew'l]trac.k~}ositi[)xl, which translates directly into an error in knowledge of the time of closest approach. AONS is therefore designed to estimate the actual time of closest approach. Critical science observations that take place within 1-2 hours of closest approach will have been designed assuming a small uncertainty in this estimate. The geometry assumed in these designs can be restored by simply shifting the start time of the observations so that they happen at the correct time relative to the actual time of closest approach. AONS will compute the appropriate time shift from the locations of Pluto and background star images in the OPNAV pictures. It will then apply the appropriate time shift to designated block(s) of science observations. This scenario is illustrated in Figure 2.

SYSTEM ARCHITECTURE

The prototype design for AONS has four primary components, or blocks. Each OPNAV picture is analyzed by the Image Processing Mock. Pluto and star images are identified and their center locations are calculated. The image centers are the navigation observable needed to solve for the time of closest approach. These observable are passed to the Orbit Determination Solution Mock that computes an update to the time of closest approach. The new estimated time is, in turn, passed to the Science Sequence Update block which determines and applies the appropriate time shift to the start time of encounter science observations. The system also includes a Geometry Update block that executes before the other three blocks. information from the previous solution (if any) is used to update the predicted spacecraft-Pluto geometry for the current picture, The new geometry information is passed to the Image Processing Mock where it is incorporated into the predictions of the appearance and location of the Pluto and star images. Figure 3 depicts this high-level system architecture and illustrates the information flow between the major Mocks.

The functions of the first three blocks executed by AONS correspond to major steps in traditional ground-based navigation procedures. Geometry Update represents the concept of keeping the nominal solution close enough to the actual solution that a linear approximation remains valid. Image Processing and Orbit Determination Solution perform the same functions, albeit in a less sophisticated manner, than the ground-based counterparts for which they are named. The Science Sequence

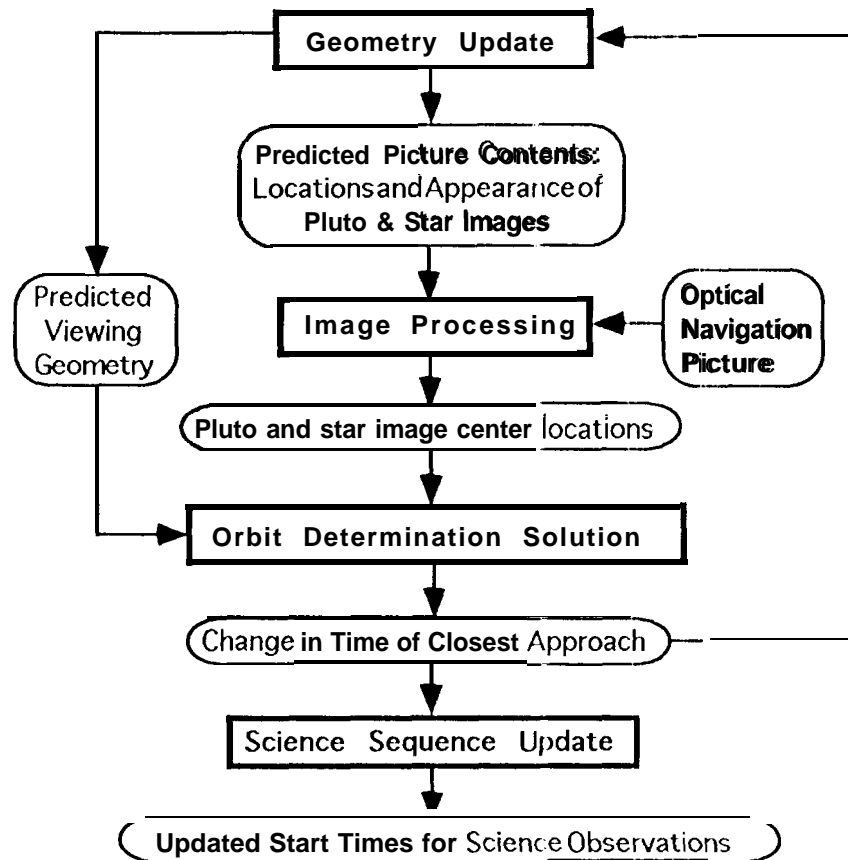


Figure 3: Functional flow chart for AONS

Update block, on the other hand, falls outside of the traditional navigation task. Furthermore, implementation of its functions is intimately tied to the design of the overall spacecraft command and control system. For these reasons, this block will not be discussed further in this paper. The next section will describe the functionality built into the three navigation-related blocks for the prototype system.

PROTOTYPE SYSTEM IMPLEMENTATION

Implementations of the Geometry Update, Image Processing, and Orbit Determination blocks for the prototype AONS are presented below. The choice of algorithms should be considered within the context of an overall design philosophy which emphasizes simplicity. Particular conditions of a Pluto flyby mission are exploited to reduce complexity of the on-board algorithms and procedures. Since Pluto is expected to have a regular (nearly spherical) shape, basic edge detection techniques are applied to find the center of the Pluto image in Image Processing. The "bootstrapping" introduced in Geometry Update limits the differences between predictions of Pluto image appearance and its actual appearance so that these algorithms remain applicable. The assumption of a linear trajectory substantially simplifies the computations in Orbit Determination Solution. The traditional multi-parameter filter is reduced to a single cubic equation giving the change in time of closest approach as a function of the difference between the actual and predicted Pluto image center locations.

The remainder of this section consists of an explanation of some background concepts that are central to the operation of AONS followed by discussions of each of the three major blocks. The descriptions of the algorithms applied in each Mock are necessarily brief; more detailed explanations and complete derivation of equations can be found in (Ref. 2).

Background Concepts

Two fundamental concepts from ground-based optical navigation theory must be presented to facilitate subsequent explanation of the operations of AONS' major blocks. The following paragraphs first discuss the mathematical representation of the image data and then derive the geometrical relationship between an object's location in inertial space and the location of its image in the O1'NAV picture.

The spacecraft's camera has a rectangular light-sensing target, assumed to be a CCD for the Pluto missions. This target is divided into a two-dimensional grid of elements called pixels. Mathematically, a picture consists of an array of values representing the intensity of light hitting each pixel. An element in this array is called a DN value and is denoted $DN(p, l)$. The coordinates (p, l) give the location of the pixel in the two-dimensional grid. Tile origin for these coordinates is the upper left corner of the picture. The horizontal coordinate, p , is positive to the right and is called the pixel (or sample) coordinate. The vertical coordinate, l , is positive downward and is called the line coordinate.

The calculation of pixel and line coordinates in a picture corresponding to the centers of optical targets such as Pluto and the background stars is repeated several times in AONS. The first step in this calculation determines camera pointing direction in the inertial reference frame. Camera body coordinates, called TV coordinates, are introduced to represent the orientation of the camera axes with respect to inertial coordinates. The z axis of TV coordinates points outward along the camera's boresight. The boresight is defined as an axis normal to the light-sensing target, or image plane, piercing the target at the center of the picture. The x and y axes of TV coordinates lie in the image plane and are parallel to the pixel and line axes, respectively. Camera pointing is represented by a set of three Euler angles describing the rotation from inertial axes to the TV coordinate axes. The commanded pointing angles are input to AONS along with the desired picture time. These angles are used to construct a transformation matrix from inertial to TV coordinates, $TITV$.

Let u represent the line-of-sight vector from the spacecraft to Pluto or a star in inertial coordinates at the time the picture is shuttered. Nominal values for u will be provided to AONS from the last ground-based trajectory solution. To find the pixel and line location, (p, l) , corresponding to u , first express u in TV coordinates

$$u_{TV} = TITV u = \begin{pmatrix} u_{TV}(1) \\ u_{TV}(2) \\ u_{TV}(3) \end{pmatrix} \quad (1)$$

Next, apply the gnomonic projection and appropriate scaling factors^{3, 4} to obtain

$$\begin{pmatrix} p \\ l \end{pmatrix} = \frac{f K_x}{u_{TV}(3)} \begin{pmatrix} u_{TV}(1) \\ u_{TV}(2) \end{pmatrix} + \begin{pmatrix} p_0 \\ l_0 \end{pmatrix} \quad (2)$$

where

- f = Focal length of the Pluto spacecraft camera.
- K_x = Scale factor for the Pluto spacecraft camera that converts from rectangular coordinates in the focal plane to pixel and line coordinates in a picture.
- p_0, l_0 = Location of the optical axis (boresight) of the Pluto spacecraft camera in pixel and line coordinates.

Eqs. (1) and (2) will appear several times in the following sections 011 the Geometry Update and Orbit Determination Solution blocks.

Geometry Update

The Geometry Update block first computes an updated value for the vector from the spacecraft to Pluto in inertial coordinates at tile time of the current picture, \mathbf{x}^U . The last ground-based navigation solution supplies nominal values for the vector from the spacecraft to Pluto at the time of each scheduled OPNAV picture, \mathbf{x}^N , and for the time of closest approach, T . The Orbit Determination Solution block supplies a value for the total change in the time of closest approach from its nominal value, ΔT , after processing the previous picture. (ΔT is set to zero for the first picture processed by AONS.) Under the assumption of a linear trajectory, the spacecraft's asymptotic approach velocity vector, \mathbf{V}_∞ , remains constant so that the updated value for tile spacecraft- Pluto vector is simply

$$\mathbf{x}^U = \mathbf{x}^N + \mathbf{V}_\infty \Delta T \quad (3)$$

Geometry Update next computes predictions for the locations of the Pluto and star image centers in the OPNAV picture. The commanded camera pointing angles are used to compute $\mathbf{T}^N \mathbf{x}^U$ is substituted for u in Eqs. (1) and (2) to obtain the updated prediction for the Pluto image center:

$$\begin{pmatrix} p_p^U \\ l_p^U \end{pmatrix} = \frac{f K_x}{x_{TV}^U(3)} \begin{pmatrix} x_{TV}^U(1) \\ x_{TV}^U(2) \end{pmatrix} + \begin{pmatrix} p_0 \\ l_0 \end{pmatrix} \quad (4)$$

A similar computation is performed to obtain (p_s^N, l_s^N) for each of the star images using its right ascension and declination coordinates to compute a vector \mathbf{u} that points towards the star. Predicted locations for the star images are passed to Image Processing as an array of offset vectors from the predicted Pluto image center. The array contains differential coordinates $\Delta p_s = p_s^N - p_p^U$ and $\Delta l_s = l_s^N - l_p^U$ for each star image.

The final computation in Geometry Update is the construction of a template representing the shape of the lit limb for the Pluto image. The template is generated as an array of offset vectors from the predicted Pluto image center to points on the lit limb of the Pluto image. The array contains differential coordinates $\Delta p_{ll} = p_{ll} - p_p^U$ and $\Delta l_{ll} = l_{ll} - l_p^U$ for a set of points $\{(p_{ll}, l_{ll})\}$ along the lit limb of the Pluto image. The calculation of the points in this array is simplified by the assumption that Pluto has a regular shape, namely that of a triaxial ellipsoid. Size information for the ellipsoid along with information on its orientation in inertial space at the time of each OPNAV picture are input to AONS. The calculation of coordinates (p_{ll}, l_{ll}) for points along the lit limb of an ellipsoid image closely follows standard limb scanning algorithms used in ground-based software.⁴ Slight modifications have been made to allow "scanning" in horizontal lines across the image so that the line coordinate of each point in the template array differs from that of the previous point by a fixed increment. The shape of the lit limb is captured by the variation in the pixel coordinate of successive elements in the template array.

Image Processing

The Image Processing block is the only part of AONS that directly accesses the image data for the current OPNAV picture. It examines the relative values of the elements in the array $DN(p, l)$ to determine the regions containing the Pluto and star images. For these later pictures, the Pluto image appears as a large crescent extending over many pixels in the picture. The star images, in contrast, are point-source images covering only a few pixels in the picture. Image Processing first searches for and locates the larger, more obvious Pluto image. It then searches for the smaller, less evident star images using information from Geometry Update on their positions relative to the Pluto image.

The procedure for locating the Pluto image is a very basic example of edge detection techniques that have long been applied in various types of image analysis. It is predicated on the assumption that the Pluto image is much brighter than the background field, including the star images, and that it extends over a significant fraction of the total picture area. AONS' edge detection algorithm examines each (horizontal) line in the current picture searching for a segment of at least W^T contiguous pixels

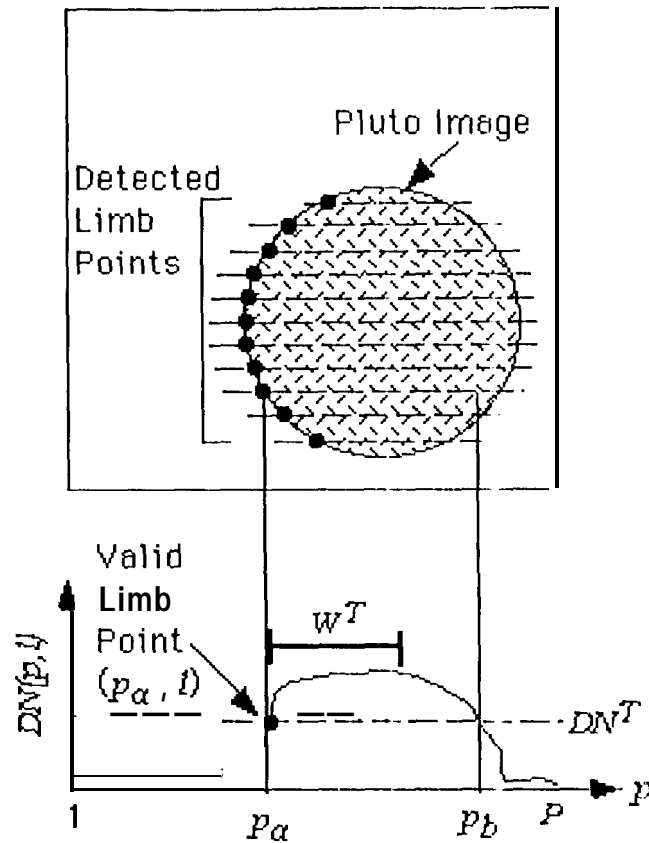
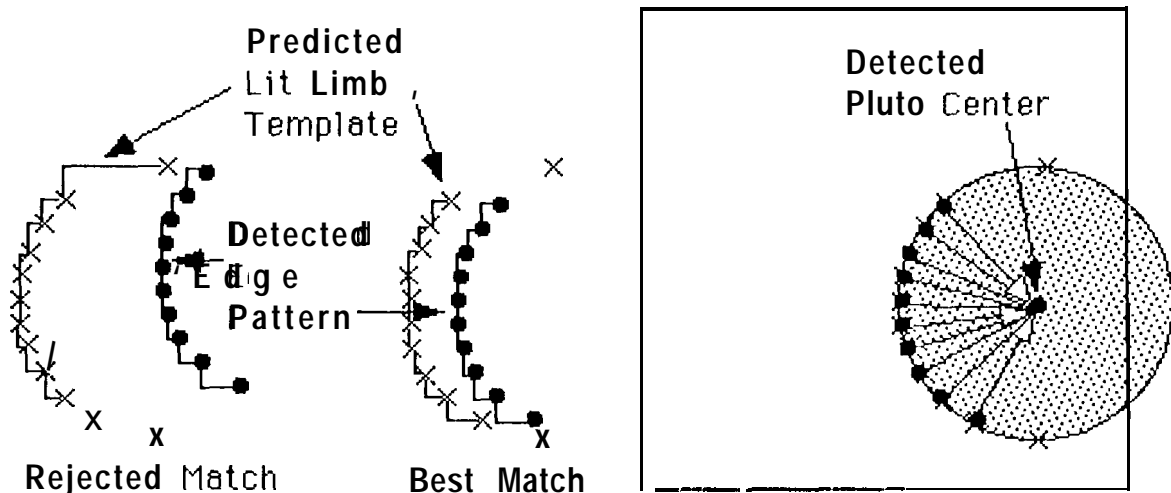


Figure 4: AONS' edge detection algorithm as applied in **Image Processing**. (p_α, l) is an entry in the array $\{(p_e, l_e)\}$.

where the brightness value $DN(p, l)$ exceeds a specified threshold value DN^T . The ends of this segment are the detected edge points. The left endpoint is considered to be a valid lit limb point (p, l_e) .[§] The picture is examined from top to bottom to generate a complete set of detected lit limb points, or edges. This process is depicted in Figure 4. The values for W^T and DN^T are supplied to AONS based on the commanded exposure time for each OPNAV picture and the expected size of tile Pluto image at that time.

The array $\{(l_e)\}$ of detected edges provides a rough estimate of the location of the Pluto image in the picture. For navigation purposes, the center of this image must be extracted from this more general information. AONS computes the Pluto image center location by comparing the general shape of the limb embodied by the points in $\{(p_e, l_e)\}$ with the predicted shape obtained from Geometry Update as the array $\{(\Delta p_{li}, A_{li})\}$. The algorithm matches every possible set of points from the lit limb template with a corresponding set of detected edges where the correspondence is determined by the pattern of vertical offsets of sequential detected edges. It computes the inner product of a vector whose elements are the horizontal offsets of consecutive points in the detected edge array with a vector of the corresponding offsets for consecutive points in the lit limb template. The location where this inner product is maximum is taken as the best match between the predicted and actual Pluto limb shapes. This process is illustrated in Figure 5(a).

[§] Camera pointing is controlled such that the lit limb points are guaranteed to fall on the left side of the Pluto image.



(a) Comparison of possible matches between detected edges and points in the lit limb template.

(b) Pluto image center is located by averaging offset vectors from the lit limb template.

Figure 5: The Edge Template Matching Process

For each point in the detected edge array, the corresponding point in the lit limb template at the best match location provides an offset vector from the Pluto center to the edge of the image. This offset is subtracted from the actual detected edge location, giving $(p_e - \Delta p_{ll}, l_e - \Delta l_{ll})$ as one possible value for the Pluto image center. This is repeated for every set of corresponding template and detected edge points in the best match. The average of these possible center values is taken as the detected center of the Pluto image, (p_P, l_P) . This is illustrated in Figure 5(b).

The final step in **Image Processing is the location** of the star images. This is accomplished by applying a well-known obvolution procedure called "box filtering" ^{5, 2} for each of the stars predicted to appear in the current OPNAV picture. First, the predicted star center is updated by adding the offset vector $(\Delta p_s, \Delta l_s)$ from Geometry Update to the actual Pluto image center (p_P, l_P) . Then, a search is made in a rectangular box around the new predicted center $(p_P + \Delta p_s, l_P + \Delta l_s)$ for the actual star image. The search consists of a comparison of subsets of brightness values, $DN(p, l)$, within the box with a template representing the brightness pattern for a point source image. The detected star image center is computed from the location of the best match with the point-source template within the search box. The width and height of the search boxes and the point-source image template are input to AONS based on the magnitudes of the stars, exposure times for each picture, and the characteristics of the Pluto spacecraft's camera.

Orbit Determination Solution

The Orbit Determination Solution Mock converts the image observables (p_P, l_P) and $\{(p_s, l_s)\}$ from Image Processing into information on the spacecraft's Pluto-relative trajectory. The star background ties the Pluto image location to the inertial reference frame of the spacecraft's equations of motion. Mathematically this relationship is captured in the TITV transformation matrix introduced earlier. The first step in Orbit Determination Solution is the calculation of an updated value $TITV^U$ based on the actual star image centers $\{(p_s, l_s)\}$. The offsets $\{(p_s - p_s^N, l_s - l_s^N)\}$ from the predicted star centers are input to a least-squares estimator to compute updated values for the camera pointing angles which are then used to construct $TITV^U$. The second step in this block is the computation

of an incremental change in the time of closest approach based on the observed shift in the Pluto image center location from its predicted value. The derivation of this relationship is presented in the following paragraphs.

The predicted Pluto center' (p_P^U, l_P^U) is computed from Eq. (4) except that x^U is converted to TV coordinates using TITV^U. The actual image center location is related to a change in time of closest approach by once again invoking the assumption of a linear trajectory. The actual spacecraft position is written as

$$x_{TV} = x_{TV}^U - t V_{\infty TV} \delta T \quad (5)$$

where x^U is computed in Geometry Update, V_{∞} is the constant approach velocity and both have been transformed to TV coordinates using TITV^U. δT represents an incremental change in the time of closest approach from its last computed value. (ΔT in Eq. (3) represents the total change in the time of closest approach from its nominal value.) Now using Eq. (2),

$$\begin{aligned} \begin{pmatrix} p_P \\ l_P \end{pmatrix} &= \frac{f K_x}{x_{TV}(3)} \begin{pmatrix} x_{TV}(1) \\ x_{TV}(2) \end{pmatrix} + \begin{pmatrix} p_0 \\ l_0 \end{pmatrix} \\ &= \frac{f K_x}{x_{TV}^U(3) + V_{\infty TV}(3)\delta T} \begin{pmatrix} x_{TV}^U(1) + V_{\infty TV}(1)\delta T \\ x_{TV}^U(2) + V_{\infty TV}(2)\delta T \end{pmatrix} + \begin{pmatrix} p_0 \\ l_0 \end{pmatrix} \\ &= \frac{f K_x}{x_{TV}^U(3) + V_{\infty TV}(3)\delta T} \left\{ \begin{pmatrix} x_{TV}^U(1) \\ x_{TV}^U(2) \end{pmatrix} + \delta T \begin{pmatrix} V_{\infty TV}(1) \\ V_{\infty TV}(2) \end{pmatrix} \right\} + \begin{pmatrix} p_0 \\ l_0 \end{pmatrix} \quad (6) \end{aligned}$$

where (p_P, l_P) is the detected Pluto center from Image **Processing**. In order to express (p_P, l_P) as the sum of (p_P^U, l_P^U) and some correction terms that are functions of δT , the term $1 / (x_{TV}^U(3) + V_{\infty TV}(3)\delta T)$ is expanded in a Taylor series about the point $\delta T = 0$. Substituting the terms up to third order in δT from the series expansion into Eq. (6) and rearranging gives:

$$\begin{aligned} \begin{pmatrix} p_P \\ l_P \end{pmatrix} &= \begin{pmatrix} p_P^U \\ l_P^U \end{pmatrix} - \frac{f K_x}{x_{TV}^U(3)} \left(\delta T - \frac{V_{\infty TV}(3)}{x_{TV}^U(3)} \delta T^2 + \frac{(V_{\infty TV}(3))^2}{(x_{TV}^U(3))^2} \delta T^3 \right) \\ &\quad \left\{ \begin{pmatrix} V_{\infty TV}(1) \\ V_{\infty TV}(2) \end{pmatrix} - \frac{V_{\infty TV}(3)}{x_{TV}^U(3)} \begin{pmatrix} x_{TV}^U(1) \\ x_{TV}^U(2) \end{pmatrix} \right\} \quad (7) \end{aligned}$$

The second term on the right in Eq. (7) is the shift in the Pluto image center due only to a change in the time of closest approach. This shift occurs in the direction represented by the vector

$$c = \frac{f K_x}{x_{TV}^U(3)} \left\{ \begin{pmatrix} V_{\infty TV}(1) \\ V_{\infty TV}(2) \end{pmatrix} - \frac{V_{\infty TV}(3)}{x_{TV}^U(3)} \begin{pmatrix} x_{TV}^U(1) \\ x_{TV}^U(2) \end{pmatrix} \right\} \quad (8)$$

Given the characteristics of the nominal trajectory solution provided to AONS, it is assumed that center shifts normal to c are negligible and that shifts along c are due only to changes in the time of closest approach. Introduce the center shift, or residual, vector

$$\begin{pmatrix} \Delta p_P \\ \Delta l_P \end{pmatrix} = \begin{pmatrix} p_P \\ l_P \end{pmatrix} - \begin{pmatrix} p_P^U \\ l_P^U \end{pmatrix} \quad (9)$$

and rewrite Eq. (7) as

$$\left(\delta T - \frac{V_{\infty TV}(3)}{x_{TV}^U(3)} \delta T^2 + \frac{(V_{\infty TV}(3))^2}{(x_{TV}^U(3))^2} \delta T^3 \right) c \cdot \begin{pmatrix} \Delta p_P \\ \Delta l_P \end{pmatrix} = 0$$

A cubic equation for δT is obtained by taking the inner product of this equation with the vector c :

$$c^2 \left(\frac{(V_{\infty TV}(3))^2}{(x_{TV}^U(3))^2} \delta T^3 - \frac{V_{\infty TV}(3)}{x_{TV}^U(3)} \delta T^2 + \delta T \right) - \begin{pmatrix} \Delta p_P \\ \Delta l_P \end{pmatrix} \cdot c = 0 \quad (10)$$

where $c^2 = c \cdot c$. Orbit Determination Solution computes δT as the sole real root of the cubic using a standard analytic formula.²

An update to the total change from the nominal closest approach time is computed by adding δT , the root of the cubic, to the previous value of AT. The new value for ΔT is stored for use in Geometry Update when the next OPNAV picture is processed.

PERFORMANCE ASSESSMENT

The prototype AONS design described in the preceding section has been implemented and tested as an extension of the navigation analysis software development system. Performance results for one sample Pluto flyby trajectory are given below. The nominal trajectory for this sample flyby was the proposed baseline for the PlutoFast Flyby mission in March of 1994. AONS was tested by generating a "true" trajectory slightly perturbed from the nominal one. The perturbations were chosen based on the expected accuracy of a ground-based orbit determination solution including optical observations up to 3 days before closest approach. OPNAV pictures were simulated using the true trajectory and processed by AONS to estimate the actual time of closest approach.

Figure 6 presents the nominal and perturbed, or true, trajectory characteristics in the navigation II-plane.⁶ The nominal trajectory is characterized by an approach velocity of 17.712 km/sec with a II-plane aimpoint of -12050 km along the T axis and 8940 km along the R axis. Closest approach occurs at 12:48:00 UTC on April 20, 2006 with the spacecraft at a distance of 15000 km from Pluto. OD accuracy at 3 days before closest approach is illustrated by the 1σ B-plane error ellipse centered on the nominal aimpoint and the 1σ error bar around the nominal time of closest approach. Also shown in the figure are the B-plane aimpoint and time of closest approach selected for the true trajectory. The D-plane aimpoint is shifted outward along the B vector by a distance of 10 km (0.80), while the time of closest approach is moved 200 sec (1 u) earlier than the nominal time.

A picture schedule for AONS was selected from opportunities predicted for the nominal trajectory. OPNAV pictures were simulated assuming that the spacecraft's camera used a CCD of 1024x 1024 pixels, each of size $10\mu\text{rad}$, for a total field-of-view of 0.5° . An albedo model for Jupiter's satellite Ganymede was scaled to an ellipsoid of Pluto's estimated size to produce brightness variations on the Pluto images. The actual spacecraft-Pluto geometry was taken from the true, or perturbed, trajectory. The star images were generated from a point-source model for the solid state imaging instrument carried by the Galileo spacecraft. Small, random pointing errors were introduced in each picture to simulate attitude control accuracy. The pointing errors introduced a uniform shift in the Pluto and star image centers while the trajectory perturbation introduced an additional shift of the Pluto image location relative to the star images. The size of the Pluto image also varied slightly due to the trajectory perturbations.

The full test suite consisted of six pictures taken between 15 and 2 hours before the nominal closest approach. Performance results will be presented for an abbreviated case where only two pictures are processed, one at the beginning and the other near the end of this period. Spacecraft range to Pluto and Pluto image diameter for these two pictures are listed in Table 1. These same values for the last ground-based picture taken 2 days earlier are also shown for comparison.

Numerical results from **Image Processing and Orbit Determination Solution** for these two pictures are summarized in Table 2. The true values for the image centers and time of closest approach and the errors in the corresponding values computed by AONS are also shown. A graphical representation of the Image Processing results for the first picture is shown in Figure 7. The simulated image is shown as the background with various overlays indicating the steps in **Image Processing**. The yellow overlays indicate the predicted image locations for the nominal trajectory and camera pointing. The green overlays are predicted lit limb and terminator points. The red overlays are the detected lit limb points and the corresponding points on the lines where the DN value falls below the threshold DN^T .

⁶This corresponds to values of $K_x = 136.53$ pixels/mm, $f = 750$ mm and $p_0 = l_0 = 512$ for the camera parameters introduced in Eq. 2.

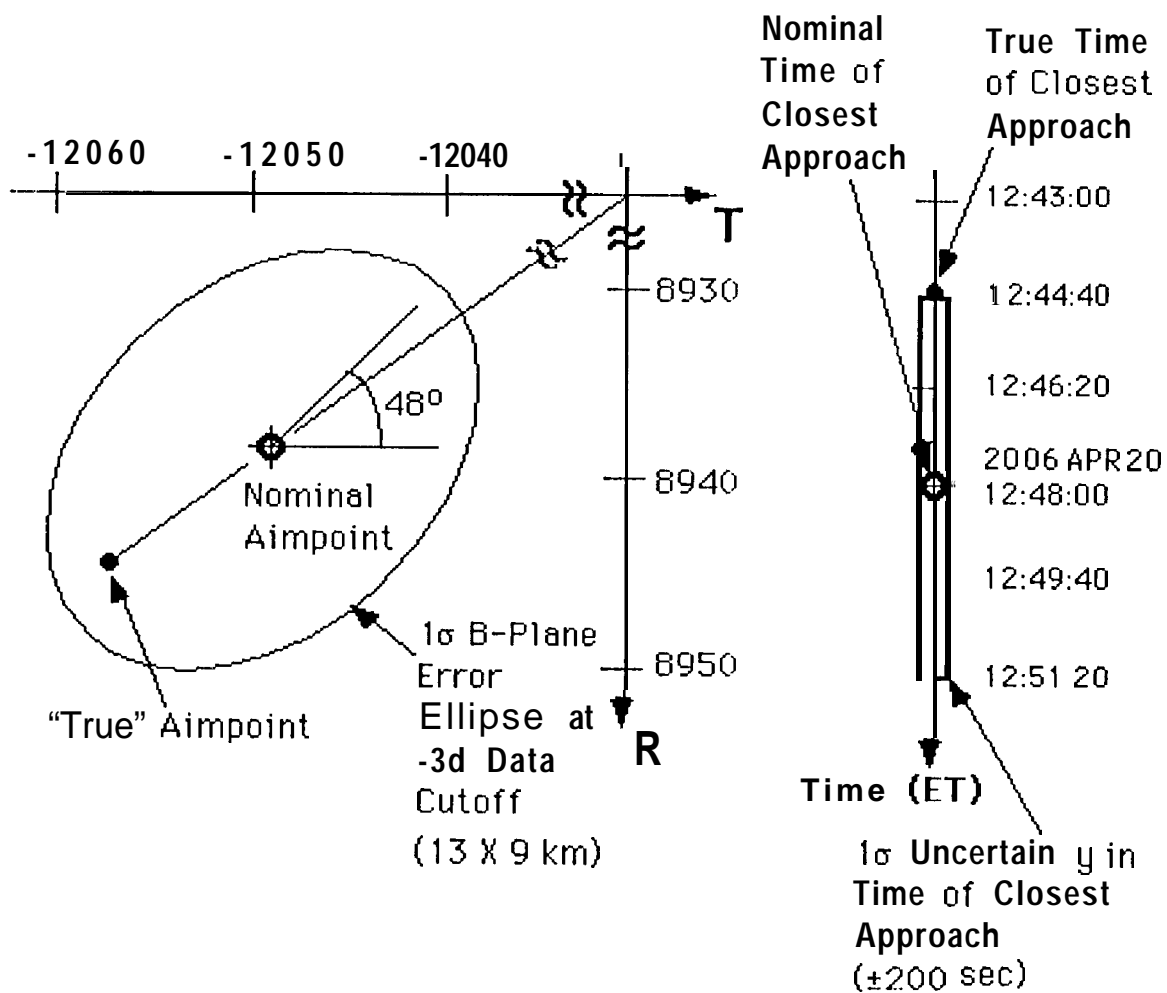


Figure 6: B-Plane targets and time of closest approach for nominal and perturbed trajectories

Event	Time from Nominal Closest Approach	Range to Pluto (km)	Pluto Image Diameter (pixels)
Ground Data Cutoff	-3 days	4637298.0	50.8
First Picture for AONS	-14.7 hours	939114.0	250.8
Second Picture for AONS	-3.7 hours	238067.0	989.3

Table 1: Spacecraft-Pluto range and Pluto image diameters for simulated OPNAV pictures

Picture Time* (hrs)	Actual Pluto Center		Detected Pluto Center		Error	
	Pixel (pixels)	Line (pixels)	Pixel (pixels)	Line (pixels)	Pixel (pixels)	Line (pixels)
-14.7	799.052	762.025	798.67	762.00	0.382	0.025
-3.7	477.163	-171.990	477.87	-174.00	0.707	-2.01

Picture Time* (hrs)	Actual Star Centers		Detected Star Centers		Error	
	Pixel (pixels)	Line (pixels)	Pixel (pixels)	Line (pixels)	Pixel (pixels)	Line (pixels)
-14.7	185.945	161.177	185.97	161.10	0.025	-0.077
	918.798	104.523	918.87	104.54	0.072	0.017
-3.7	258.922	312.519	258.96	312.55	0.038	0.031
	790.734	917.043	790.83	917.02	0.096	-0.023

Picture Time* (hrs)	Estimated Time of Closest Approach (ET)	Error (sec)
-14.7	2006 APR 20 12:43:51.4	-48.6
-3.7	2006 APR 20 12:44:31.2	-8.8
Actual Closest Approach	2006 APR 20 12:44:40.0	

*Picture times given as hours before the *nominal* closest approach time of 2006 APR 20 12:48:00 ET.

Table 2: Detected image centers and time of closest approach estimates from AONS

The green overlays are drawn over the red overlays to indicate the best match between the lit limb template and the detected limb points. Only the overlays on the left of the Pluto image are used in determining the best match- they are the lit limb template and the detected limb points. The red and green overlays on the right are predicted and detected terminator points which are not used in Image Processing. The red cross in the center of the Pluto image indicates the center location calculated by **Image Processing**. The blue boxes and crosses at their centers indicate the predicted star locations and the search areas for the box filtering algorithm. The red crosses indicate the locations within the search areas where the actual star images are found. The star images themselves are too small to be visible under these overlays.

Figure 8 illustrates the **Science Sequence Update** step applied to a representative near encounter science observation. The sample observation consists of a series of 10 frames running from the terminator to the lit limb in the mid-section of the Pluto image and is scheduled to begin at 5 minutes before the nominal closest approach time. Figure 8(a) shows the ideal design where pointing angles and start time are chosen for the nominal trajectory. Figure 8(b) shows the same design with the Pluto image in its correct location for the perturbed (or true) trajectory. Without the AONS updates, this observation will entirely miss its target. Figure 8(c) shows the mosaic design using the nominal pointing angles but with its start time shifted by the amount computed from AONS' processing of the first picture. A few of the frames are now capturing part of the Pluto image. The design moves even closer to the ideal case after AONS' update from the second picture as shown in Figure 8(d). The background grids in the figure represent right ascension and declination coordinates on the celestial sphere. The grid lines and mosaic frames always appear in the same location since camera pointing angles are not modified by AONS.

The performance results presented above have been verified by implementation and testing of the prototype system in the Flight System Testbed (FST) at JPL. The FST provides a flight-like environment using both software tools and actual flight hardware to simulate spacecraft operation.

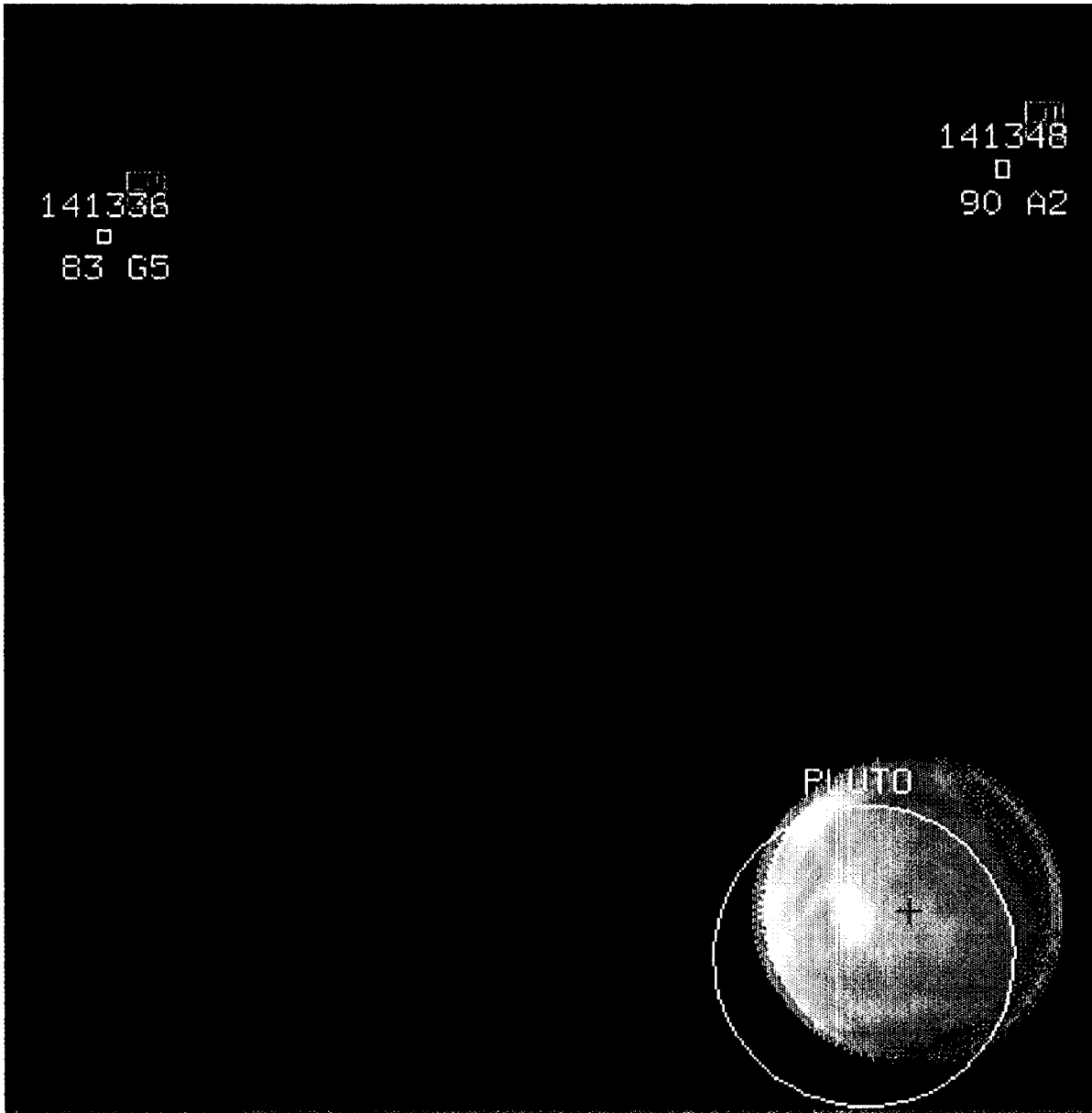
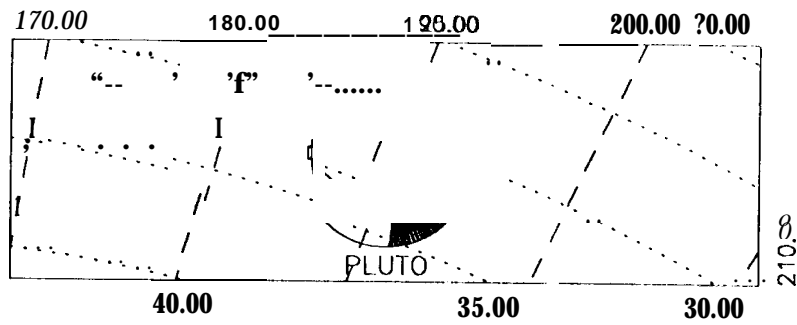
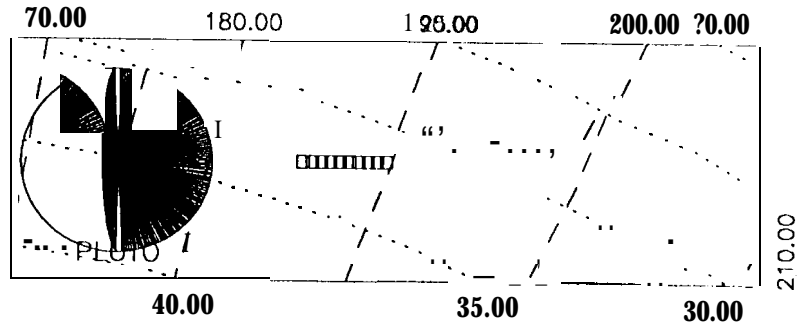


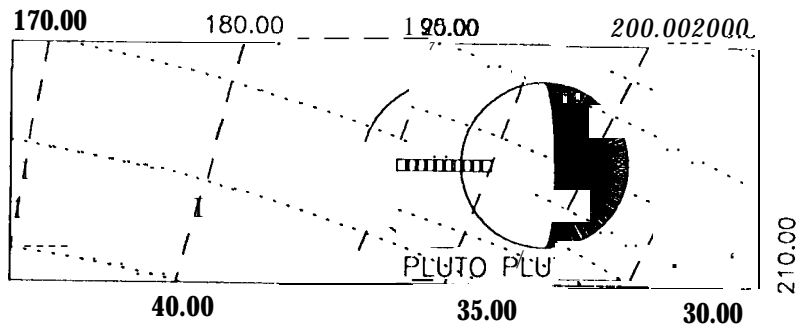
Figure 7: AONS' image processing results for the picture taken 15 hours before the nominal closest approach.



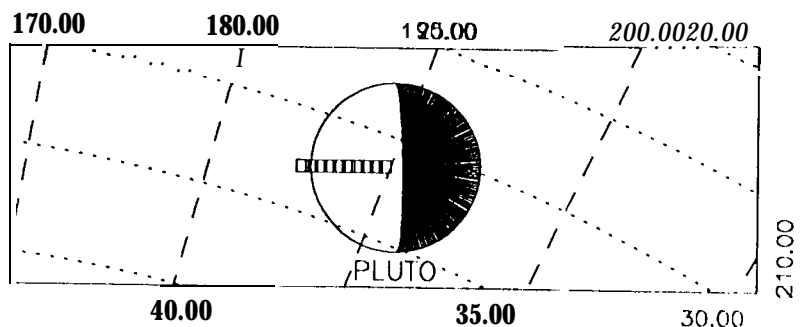
(a) original mosaic design for nominal trajectory.



(b) Mosaic fails to capture Pluto for the true trajectory without start time updates from AONS.



(c) Some of the mosaic frames capture Pluto after the first start time update from AONS.



(d) Most of the mosaic frames capture Pluto after the second start time update from AONS.

Figure 8: Updates to sample science observation using AONS' solutions for time of closest approach

Successful testing of AONS in FST provides confidence that a flight-qualified version can be developed to meet a proposed requirement of less than 10 seconds uncertainty in the estimated time of closest approach when the last OPNAV picture is taken and processed at about 4 hours before closest approach.

Future Development

Much work remains to be done to evolve the prototype AONS to a flight-qualified system. The prototype demonstrates only the most basic functionality and was designed with poor knowledge of desired performance requirements. Formal performance requirements that satisfy mission objectives should be determined by engineering and science teams. The prototype design can then be evaluated in the framework of those requirements to identify the necessary modifications. Some areas of concern and the changes that they may impose on the system are discussed in the following paragraphs.

One of the simplifying assumptions for the prototype system is that the OPNAV picture times are selected and programmed into the spacecraft encounter sequence based on the best available ground-based trajectory. For the worst-case downtrack errors, the Pluto image may shift far enough from its nominal predicted locations that it is not captured in some of these OPNAV pictures. The tacit assumption has been that a sufficient number of successful observations can be guaranteed by adding some extra opportunities to a baseline picture schedule. This strategy has not been considered in detail nor have any test cases been run to demonstrate its validity. If this strategy is not adequate, it may be necessary to add a picture planning function to AONS. This function would continuously evaluate OPNAV picture opportunities and implement observations as they occur during the encounter. This would significantly increase system complexity since it requires greater interaction and coordination with other spacecraft control functions. With or without the picture planning function, error handling will have to be added to the basic system to allow it to identify and eliminate any missed observations.

Like the worst-case downtrack errors, worst-case shifts in the B-plane aimpoint can also cause problems. The assumption that the observed shift in the Pluto image center can be attributed entirely to a change in the time of closest approach may not be valid under these circumstances. The contribution of shifts in the B-plane aimpoint should be analyzed to determine if they should be considered in the orbit determination solution. The single cubic equation could be replaced with a three-parameter lewd-squares filter that estimates B-plane aimpoint coordinates as well as the time of closest approach. This filter could improve the accuracy of the estimation of the time of closest approach by isolating it from contributions due to B-plane shifts.

The centerfinding procedures in **Image Processing** should be more carefully evaluated. The algorithms for Pluto and star images need to be tested on pictures including random noise characteristic of the camera in the Pluto environment. Additional routines may be required to insure that the real images can be distinguished from background noise signatures. Time constraints in AONS' development schedule caused the restriction that camera pointing be controlled to put the lit limb on the left of the Pluto images to remain in the design. It should be relatively straightforward to modify the procedure that scans horizontally for lit limb points to determine the orientation of the Pluto image in the picture frame and select the proper scan direction. This extension would be necessary if the camera pointing angle representing rotation about the boresight (the "twist" angle) cannot be actively controlled.^{||} Also, the moon Charon will be appearing in the pictures with Pluto itself until rather late in the encounter. Modifications to the centerfinding procedures are needed to handle pictures containing multiple extended body images. Finally, the basic edge detection algorithms may have to be augmented with more sophisticated algorithms if centerfinding accuracy must be reduced below 1 pixel.

Overall fault tolerance and robustness of the system were not addressed in the prototype design, but must be considered a priority for any flight system. Error handling procedures must be designed and integrated into the existing system. This includes treatment of problems within AONS' own

^{||}Full control of camera pointing, including twist angle, was part of the PFF spacecraft design.

subsystems as well as its interaction with the rest of the spacecraft flight control system. Such features have not been emphasized in ground-based navigation software due to the presence of a human analyst in the loop.

CONCLUSIONS

An autonomous optical navigation capability has been proposed to meet navigation requirements within the unique constraints of a Pluto flyby mission. A prototype design for the autonomous system has been derived from traditional ground-based navigation procedures. Its high-level architecture mimics the basic steps used in ground operations. Simplified implementations of these basic steps have been developed by exploiting the special characteristics of a Pluto mission. The prototype has been successfully tested for a sample Pluto trajectory on navigation analysis computers and in the Flight System Testbed at JPL. The system reduced the uncertainty in the time of closest approach from a few hundred seconds to approximately 1(1 seconds using optical data taken up to 4 hours before closest approach.

The migration of navigation functions to the spacecraft flight system represents a significant departure from navigation operations for previous missions. The Pluto autonomous optical navigation system is one of the first proposed uses of such technology for interplanetary missions. Successful testing of the prototype demonstrates that its design forms a good foundation for development of a true flight system should a Pluto mission be undertaken in the future. This system may also serve as a stepping stone in the development of a generic autonomous navigation capability for other types of missions. Many of the functions included in the Pluto system will also be needed in a more general system.

ACKNOWLEDGEMENT

The work described in this paper was carried out at the Jet Propulsion Laboratory, California Institute of Technology, under a contract with the National Aeronautics and Space Administration.

REFERENCES

1. R. J. Haw, C. E. Helfrich, R. . Vaughan, and B. G. Williams, "Mission to Pluto: A Navigation Assessment," paper AAS 95-113, AAS/AIAA Spaceflight Mechanics Meeting, Albuquerque, NM, February 13-16, 1995.
2. Vaughan, R. M., "Pluto Fast Flyby Autonomous Optical Navigation System Algorithm Design Document," JPL EM 314-577, October 17, 1994.
3. Vaughan, R. M., "Pluto Fast Flyby Autonomous Optical Navigation System Functional Description," JPL IOM 314.8-905, July 20, 1994.
4. Owen, W. M. and Vaughan, R. M., *Optical Navigation Program Mathematical Models*, JPL EM 314-513, August 9, 1991.
5. Donegan, A. J., Riedel, J. E., and Stuve, J. A., *The ONIPS System User's Guide*, JPL EM 314-490, August 15, 1990.
6. Taylor, A. H., Jonasescu, R., and Vaughan, R. M., "A First Look at Orbit Determination for the Cassini Mission," paper AAS 93-608, AAS/AIAA Astrodynamics Specialist Conference, Victoria, B. C., Canada, August 16-19, 1993.